ACS OMEGA

http://pubs.acs.org/journal/acsodf

Article

Density Functional Simulation Study of Surface Wettability of Coal Molecules with Different Degrees of Defects

Liyong Tian, Xiuyu Yang, Shuai Wang,* and Ning Yu

Cite This: *ACS Omega* 2022, 7, 47031−47039

Read Online

ACCESS | Metrics & More | Article Recommendations

ABSTRACT: To explore the adsorption mechanism of H_2O molecules on the surfaces of defective coal molecules and perfect bituminous coal molecules, the energy band structure, electronic density of states, electrostatic potential, and front orbitals on the surfaces of three coal molecule models were investigated using quantum chemical density functional theory (DFT) simulations. The adsorption energy and Mulliken charge layout of H_2O molecules with the surfaces of defective coal molecules and perfect bituminous coal molecules were similarly investigated. The results of the DFT calculations showed that the widths of the forbidden bands of the defective coal molecular surfaces were narrower, and the electrostatic potential values were smaller. In addition, they each had an increased conduction band near the Fermi energy level, a larger electronic density of states near the Fermi energy level, and a higher electron activity and electron density than those of the perfect bituminous coal molecular surface. While stable adsorption of H_2O molecules occurred on the surfaces of the single-vacancy-defective coal molecules, double-vacancy-defective coal molecules, and perfect bituminous coal molecules, the adsorption energy values were −39.401, −30.002, and −29.844 kJ/mol for the more stable configurations, corresponding to −0.022, −0.013, and −0.011 electrons gained by H_2O molecules, respectively. Wettability improved with the appearance of defects, and the order of improvement was single-vacancy-defective coal molecule > double-vacancy-defective coal molecule > no-defect coal molecule.

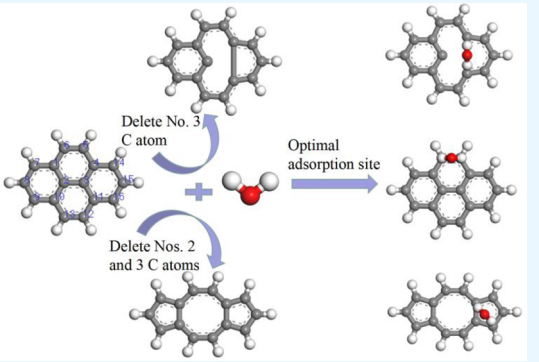

1. INTRODUCTION

Flotation is a beneficiation method that employs the difference in physical and chemical properties of a mineral surface to separate useful minerals from the vein, involving a solid−liquid−gas phase making it suitable for sorting low-grade, fine-grained leached ore and often involving the froth flotation method.[1−3] Coal is one of the most abundant and widely distributed energy sources in the world,[4] abundant in China, the United States, Russia, and Australia.[5,6] The flotation method is used to efficiently separate fine coal particles, reduce the ash content in coal particles, and remove fine sulfur iron ore from coal particles.[7]

Flotation methods utilize the principle of liquid surface tension so that while hydrophobic mineral particles attach readily to air bubbles, hydrophilic particles, which are easily wetted by water to form a hydrated film, cannot attach to the air bubbles and remain in the pulp, thus facilitating sorting.[8] The wettability of fine coal particles is an important factor in determining the success of flotation. The wettability of the coal molecule surface is mainly influenced by the grade of the coal, surface functional groups, surface electronic properties, and defects.[9,10] Low-grade coal contains more oxygen-containing functional groups: −COOH, −OH, −C═O, −O−, and H_2O molecules, which easily form hydrogen bonds, especially −COOH, and the hydration film formed prevents the fine coal particles from attaching to air bubbles.[11] Medium- and high-grade coals have fewer oxygen-containing functional groups, but the defects on the surfaces of the coal molecules enhance adsorption with H_2O molecules; thus, the coal molecules do not easily attach to air bubbles. The gain and loss of electrons on the surfaces of coal molecules affect their interaction with H_2O molecules and, consequently, the wettability of the surfaces of coal molecules. To separate hydrophilic fine coal particles, a suitable flotation agent needs to be added to improve the wettability of the coal particle surface so that it can easily adhere to the air bubbles and make sorting easier.[12]

Recent developments in density functional theory (DFT) and molecular dynamics simulation, as well as improvements in computer hardware, have enabled quantum theory and molecular simulation methods to provide effective theoretical tools for the study of adsorption properties of gases in coal

Received: September 23, 2022
Accepted: November 21, 2022
Published: December 6, 2022

seams and the calculation of surface interactions.[13−15] The application of molecular simulations to calculate coal-water adsorption, coal surface electronic properties, and wettability has been important research in the field of coal flotation.[16] Xia et al. used MD simulation to demonstrate coal-water, coal-bubble, and coal-catcher interactions and concluded that −COOH and −OH in lignite molecules could easily form hydrogen bonds with H_2O molecules to form a hydration film. The film then prevented the coal molecules from attaching to the air bubbles. After adding the catcher, the wettability of the coal surface was significantly improved, and flotation was facilitated.[17] Zhang et al. investigated the surface wettability of coals of different grades using a combination of experiments and simulations. They found that the magnitude of the degree of the contact angle was bituminous coal > anthracite > lignite, indicating that lower grade coals had greater wettability.[18] Xia et al. analyzed the effect of adding of dodecyl trimethylammonium bromide (DTAB) to the surface of low-grade coal on its adsorption characteristics by experimental methods. The results showed that the hydrophobicity of the coal surface first increased with addition of small quantities of DTAB and then later decreased as the DTAB concentration increased. The interaction between H_2O molecules and coal molecules decreased, which effectively improved the hydrophobicity of low-grade coal.[19] Wang et al. investigated the relationship between coal surface wettability and oxygen-containing functional groups at the molecular level by constructing different oxygen-containing functional groups on the coal surface and then simulating the interaction between H_2O molecules and OFGs.[20] Some research results have shown that the graphite surface is hydrophobic, whereas other results have suggested that graphite is mildly hydrophilic. Max and Zhuang et al. therefore investigated the wettability of graphite by constructing three kinds of defects on its surface: point defects, line defects, and zone defects.[21,22] Shakeri et al. explored the electronic properties of SW defects distributed on AGNR using a tight-binding model and concluded that defect density has significant effects on conductivity, band gap, and transport properties.[23] Guo et al. compared the formation energy and adsorption energy differences of molecular structural defects in tectonic coals with the help of molecular simulations to explore the formation mechanism of structural defects and simulated the adsorption behavior of gas molecules on different structural defects using the grand canonical Monte Carlo (GCMC) method.[24] del Castillo et al. used molecular simulations to reveal the effect of graphene surface defects on the adsorption properties and adsorption time stability of CO_2 molecules.[25]

There are many local and international studies on the simulation and calculation of the adsorption of different small molecules on the surfaces of coal molecules,[26−31] but the analysis of the adsorption of small molecules at the atomic and electronic level is still relatively rare. To determine the adsorption behavior of different defective coal molecular surfaces with H_2O molecules, we investigated the energy band structure, electronic density of states, electrostatic potential, and frontline orbitals of three kinds of coals: single-vacancy-defective, double-vacancy-defective, and perfect bituminous coal molecular model surfaces. The analysis utilized density functional theory to compare the interactions between H_2O molecules and coal molecular surfaces with different degrees of defects and to explore their adsorption mechanisms. The study is intended to add to our understanding of coal surface wettability and to provide a new perspective on the interfacial interactions in the flotation process of coal.

2. SURFACE MODEL AND CALCULATION METHOD

2.1. Model Construction. To analyze the effect of defects in bituminous coal molecules on the adsorption of H_2O molecules, we selected the hexacyclic aromatic cluster 2 × 2 ($C_{16}H_{10}$) to simulate the initial bituminous coal surface to be used for the quantum chemical calculations, as shown in Figure 1(a). By deleting No. 3 C atom on the surface of the initial coal molecule, dangling bonds were formed on Nos. 2, 4, and 11 C atoms, where Nos. 4 and 11 C atoms will form stable bonds, resulting in a single-vacancy-defective coal molecule surface model, as shown in Figure 1(b). By deleting Nos. 2 and 3 C atoms on the surface of the initial coal molecule, stable bonds were formed between Nos. 1 and 10 and between Nos. 4 and 11, resulting in a double-vacancy-defective coal molecule surface model, as shown in Figure 1(c).

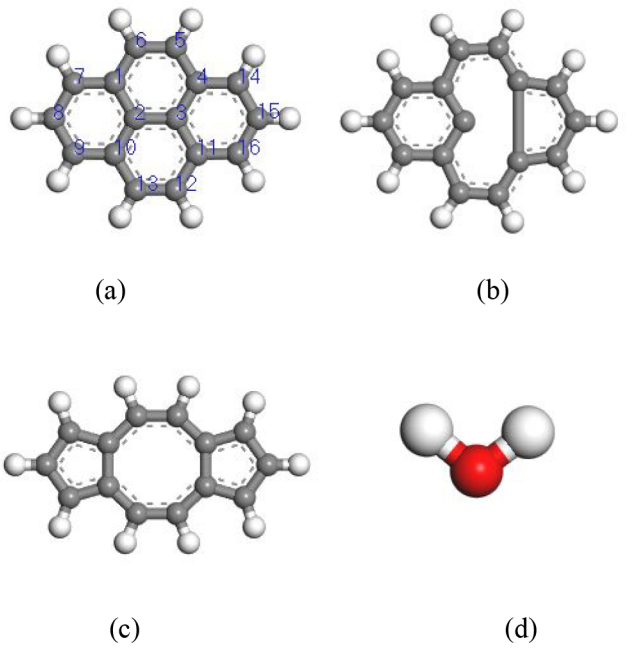

Figure 1. Geometrically optimized models of the different coal molecules and the H_2O molecule (white: H atoms; red: O atoms; gray: C atoms). (a) No-defect coal molecules, (b) single-vacancy-defective coal molecules, (c) double-vacancy-defective coal molecules, (d) H_2O molecule.

2.2. Calculation Details. Materials Studio software was used to calculate the molecular properties and optimize the initial no-defect bituminous coal molecules, single-vacancy-defective coal molecules, double-vacancy-defective coal molecules, and H_2O molecules. The $Dmol^3$ module was used for the geometric optimization of the different molecules mentioned above, and the maximum number of iterations of the geometric optimization was set at 500 to ensure its convergence. The correlation function of electron exchange adopted the Perdew−Burke−Ernzerhof (PBE) functional based on a generalized gradient approximation (GGA)[32] and used the DFT semicore pseudopots and double numeric with polarization (DNP) basis set,[33] The accuracy was set at "Fine", electron spins were unrestricted, and electronic distribution was symmetric. The convergence accuracy of the self-

https://doi.org/10.1021/acsomega.2c06146
ACS Omega 2022, 7, 47031−47039

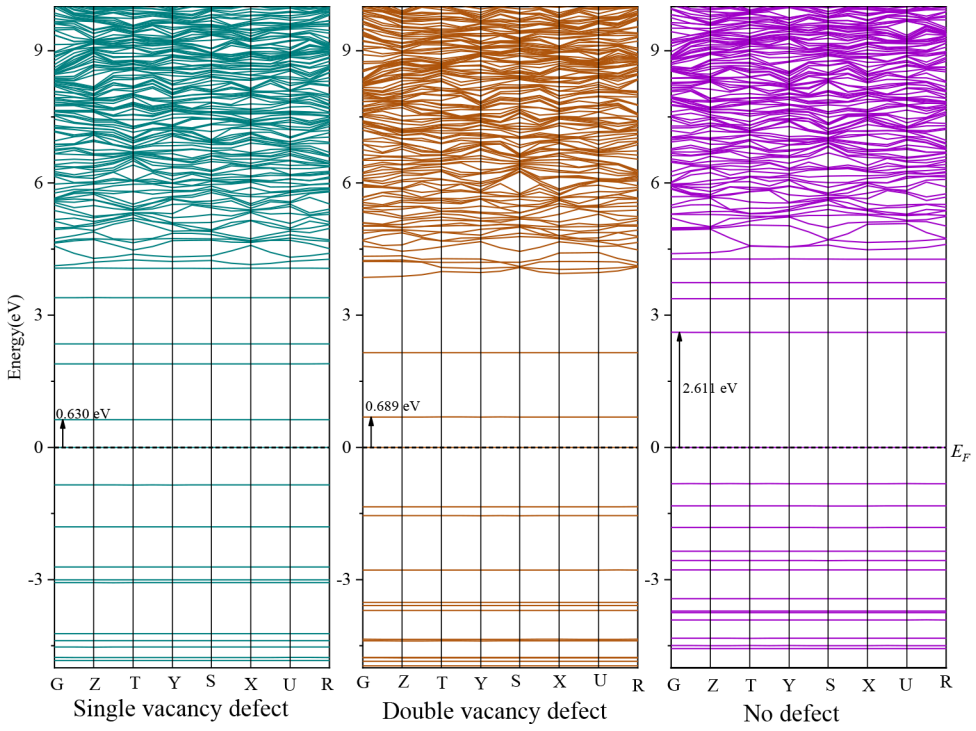

Figure 2. Energy band structure of the different coal molecules.

consistent field was set at 1.0×10^{-6},[34] max SCF cycles was set at 500, and smearing was set at 0.005 Å. The convergence criteria for geometric optimization were as follows: energy was set at 1.0×10^{-5} Ha, max. force was set at 0.002 Ha/Å, and max. displacement was set at 0.005 Å. The geometrically optimized surfaces of the different coal models and H_2O molecules are shown in Figure 1. The stable adsorption configurations of the different coal molecules with H_2O molecules were calculated using the Grimme method for DFT-D correction.

The electrostatic potential and frontline orbital properties of the different coal molecule surface models and the H_2O molecules that completed the energy optimization were calculated using the Dmol^3 module. The electrostatic potential analysis was performed by simultaneously calculating the electron density and electrostatics and then deriving the electrostatic potential map by analysis. The CASTEP module was used to calculate the energy band structure and total density of states (TDOS) of the perfect bituminous coal molecules[35] as well as the single-vacancy-defective and double-vacancy-defective coal molecules with complete energy optimization. The different coal molecules were optimized by placing them in 15 × 15 × 15 Å periodic crystals. The exchange correlation function and convergence standard were the same as those of the Dmol^3 module, and ultrasoft pseudopotentials were used to describe the interaction between the electrons and ions.[36] The high-symmetry points of the simple Brillouin zone were recorded to calculate the width of the forbidden band. Eight special high-symmetry points were selected and identified as G, Z, T, Y, S, X, U, and R. The width of the forbidden band was obtained through the energy band. The smearing value used for the TDOS analysis was 0.2 eV.

The wettability of the H_2O molecules on the surfaces of the different coal molecules can be expressed in terms of the adsorption energy. The adsorption energy is negative because this is an exothermic reaction. The lower the value, the stronger the adsorption; the more stable the adsorption, the greater the wettability, and vice versa. The calculation formula of adsorption energy is as follows:

$$E_{ads} = E_{A/B} - E_A - E_B \quad (1)$$

where E_{ads} is the adsorption energy of the H_2O molecules on the surfaces of the different coal molecules (kJ/mol); $E_{A/B}$ is the total energy of the stabilized system after adsorbing the H_2O molecules on the surfaces of the different coal molecules (kJ/mol); E_A is the energy of the different coal molecules before adsorption (kJ/mol); and E_B is the energy of the H_2O molecule before adsorption.

3. RESULTS AND DISCUSSION

3.1. Energy Band Structure Analysis. The energy band structure can reflect the surface electron leap properties of the coal molecule model. Figure 2 shows the energy band structure on the surfaces of the defective and perfect coal molecule models. As the figure illustrates, the widths of the forbidden bands of the single-vacancy-defective coal molecules, double-vacancy-defective coal molecules, and perfect bituminous coal molecules are 0.630, 0.689, and 2.611 eV, respectively, with no overlap between the valence and conduction bands. The narrower the forbidden band, the easier it is for electrons to jump from the highest occupied state to the lowest empty orbit and the less energy required for the jump. The forbidden bands of both the single-vacancy-defective and double-vacancy-defective coal molecules are narrower than that of the perfect surface, indicating that the defects affected the electronic properties of the coal molecule surface so that the electrons could jump more easily leading to enhanced adsorption of the defective coal molecules and H_2O molecules. The width of the forbidden band of the single-vacancy-defective coal molecules

https://doi.org/10.1021/acsomega.2c06146
ACS Omega 2022, 7, 47031−47039

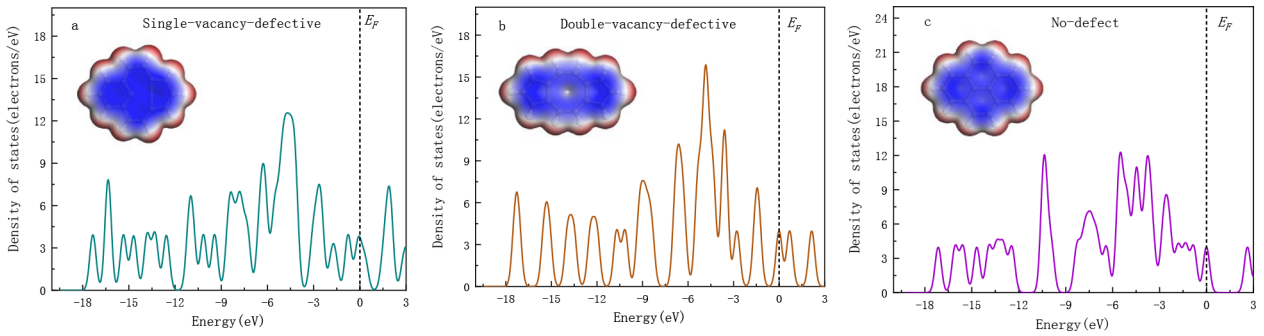

Figure 3. TDOS and electrostatic potential projections on the surfaces of the different coal molecules. (a) Single-vacancy-defective coal molecules, (b) double-vacancy-defective coal molecules, (c) no-defect coal molecules.

was narrower than that of the double-vacancy-defective coal molecules, as a result of the dangling bonds. According to energy band theory, the closer the energy band to the Fermi energy level, the stronger the ability of the valence band to lose electrons and the conduction band to gain them.[37−39] The figure illustrates that the energy bands on the surfaces of the defective coal molecules are closer to the Fermi energy level, and at 0−3 eV, the single-vacancy-defective, double-vacancy-defective, and perfect coal molecules have 3, 2, and 1 conduction bands, respectively. The increase in the conduction band indicates that the electron activity is in the order of single-vacancy defect > double-vacancy defect > no-defect, and the electrons can easily jump from the valence band to the conduction band.

3.2. Total Density of States (TDOS) and Electrostatic Potential Analysis. TDOS characterizes the relationship between the number of states and energy, reflecting the degree of electron activity; the electrostatic potential characterizes the degree of charge enrichment on the surface of the coal molecules. Figure 3 illustrates the electronic density of states and the projections of electrostatic potential on the surfaces of the different coal molecules. The greater the number of states near the Fermi energy level, the more electronically active the coal molecule surface is. The blue area in the figure illustrates the negative electrostatic potential, that is, the charge with negative electrical properties. When the color is darker, the electrostatic potential is smaller, indicating electron sufficiency. The red area in the figure illustrates the positive electrostatic potential, that is, the charge with positive electrical properties. When the color is darker, the electrostatic potential value is greater, indicating a relative lack of electrons. The TDOS plots reveal relatively sharp wave peaks with peaks of 7.38 and 4 electrons/eV occurring on the surfaces of the single- and double-vacancy-defective coal molecules, respectively, both in the 0−3 eV range of the conduction band. In contrast, only small wave peaks occur on the surfaces of the perfect coal molecules, with a peak of 3.38 electrons/eV. The higher density of states near the Fermi energy level of the defective coal molecule indicates that the electrons on the surface of defective coal molecules are more active.[40−43] The projection of the electrostatic potential shows that the smallest electrostatic potential value of the single-vacancy-defective coal molecule surface was located at the defects with a value of −0.041 au (Figure 3(a)); the smallest electrostatic potential value of the double-vacancy-defective coal molecule surface was around the five-ring aromatic cluster with a value of −0.027 au (Figure 3(b)); the smallest electrostatic potential value of the perfect coal molecule surface was around the whole 2 × 2 aromatic cluster with a value of −0.025 au (Figure 3(c)). A comparison of the magnitude of the electrostatic potential values on the surfaces of the different coal molecules reveals that the surfaces of the single-vacancy-defective coal molecules have the highest electron density. In summary, the surfaces of the defective coal molecules are more electronically active, have higher degrees of electron accumulation, interact more strongly with H_2O molecules, and utilize less adsorption energy than the surfaces of the perfect coal molecules.

3.3. Frontline Orbital Analysis. Frontline orbital theory suggests that reactants have higher reactivity in their highest occupied molecular orbitals (HOMO) and lowest unoccupied molecular orbitals (LUMO). These determine the interactions between reactants. Usually, the HOMO of one reactant reacts with the LUMO of another reactant, and the smaller the absolute value (ΔE) of the energy difference between the two, the more efficient the interaction between the reactants.[44,45] The frontline orbital energy differences between the different coal molecular models and H_2O molecules were calculated, and the results are shown in Table 1. As the table shows, $\Delta E_2 <$ ΔE_1. This indicates that the LUMOs of the different coal molecular models are able to interact efficiently with the HOMOs of the H_2O molecules. A comparison of ΔE_2 shows that the absolute value of the energy difference between the LUMO of the defective coal molecular model and the HOMO of the H_2O molecule is much smaller than that of the perfect coal molecular model, with the smallest ΔE_2 for the single-vacancy-defect coal molecule, indicating that the H_2O molecule is easily adsorbed on the defective coal molecular

Table 1. Calculated Frontline Orbital Energy Differences between the Different Coal Molecular Models and H_2O Molecules[a]

Models	Frontier orbital energies/eV		Frontier orbital energy difference/eV	
	HOMO	LUMO	ΔE_1	ΔE_2
Single-vacancy-defect	−4.125	−3.897	5.178	2.847
Double-vacancy-defect	−4.437	−3.692	5.490	3.052
No-defect	−4.992	−2.361	6.045	4.383
H_2O	−6.744	1.053	-	-

[a] ΔE_1 = |*E*coal HOMO − *E*H_2O LUMO|, ΔE_2 = |*E*H_2O HOMO − *E*coal LUMO|, where *E*coal HOMO and *E*coal LUMO are the HOMO and LUMO energies on the surfaces of the different coal molecular models, respectively; *E*H_2O HOMO and *E*H_2O LUMO are the HOMO and LUMO energies of the H_2O molecule, respectively.

https://doi.org/10.1021/acsomega.2c06146
ACS Omega 2022, 7, 47031−47039

model, especially on the surface of the single-vacancy-defective coal molecular model.

The frontline orbitals of the three coal molecule models and H_2O molecules are illustrated in Figure 4, where Figure 4(a−c)

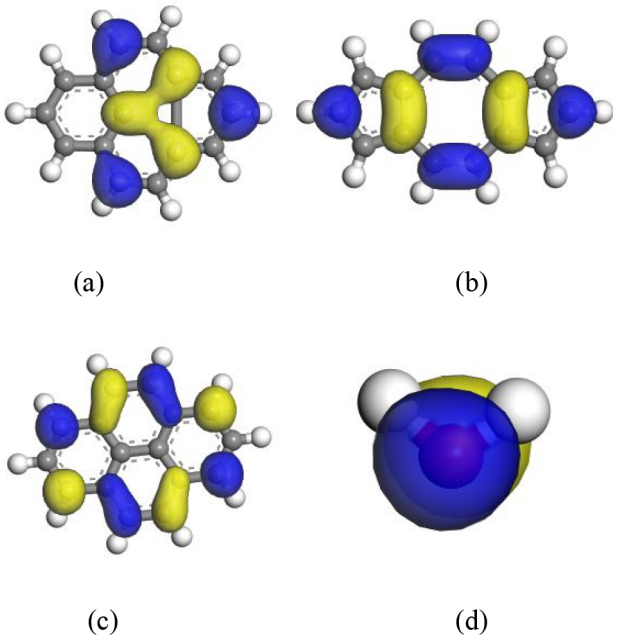

Figure 4. Frontline orbitals of the different coal molecular models and H_2O molecules. (a) Single-vacancy-defective coal molecules, (b) double-vacancy-defective coal molecules, (c) no-defect coal molecules, (d) H_2O molecule.

shows the LUMOs of the three coal molecules, respectively, and Figure 4(d) shows the HOMOs of the H_2O molecules. For a clear view of the frontline orbitals, the LUMO equivalence surfaces of the different coal molecules were taken to be 0.03 electrons/Å^3, and the HOMO equivalent surface of the H_2O molecule was taken to be 0.07 electrons/Å^3. As Figure 4 illustrates, the LUMOs of the defective coal molecules appear at the defects of the coal molecules and on the C atoms around the defects (Figure 4(a,b)), with the intensity being greatest at the defects. The LUMO of the perfect coal molecule appears on the C atom around the 2 × 2 aromatic cluster (Figure 4(c)). The HOMO of the H_2O molecule appears on the O atom (Figure 4(d)) and has the maximum intensity at this position. Therefore, the more the O atoms of the H_2O molecules tend to adsorb at the sites of the defects of the defective coal molecules and the C atoms around the aromatic clusters of perfect coal molecules, the more stable the adsorption system is.

3.4. Adsorption Energy Calculation and Charge Analysis. The adsorption of H_2O molecules occurs in two ways. First, two H atoms point toward the surface of the coal molecule model (downward); second, two H atoms point in the direction of the vacuum (upward).[46] Due to the appearance of LUMO orbitals and the deepest color of electrostatic potential projection on the defects of defective coal molecules and the C atom around the aromatic cluster of perfect coal molecules, combined with the symmetry of coal molecules, five adsorption sites were created on the surfaces of the single-vacancy-defective coal molecules and those of the perfect coal molecules, respectively (see Figure 6(a−e) and Figure 6(l−p)). In the case of the double-vacancy-defective coal molecules, six adsorption sites were created on their surfaces (Figure 6(f−k)). That is, there were 32 combinations of adsorption configurations for the adsorption mode of H_2O molecules and the model adsorption sites of coal molecules. When placing the H_2O molecule, the oxygen atom was taken as the placement center for the H_2O molecule, due to the fact that the HOMO orbital of the H_2O molecule appeared on the oxygen atom. The initial distance of the placement center of H_2O molecules adsorbed on the surface of the coal model were 3 Å. The side and top views are illustrated in Figure 5. The

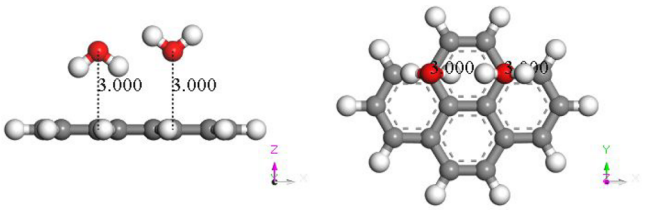

Figure 5. H_2O molecule adsorption mode (left: side view, right: top view).

initial adsorption configurations of the H_2O molecules on the surfaces of the different coal molecular models are illustrated in Figure 6 (only the adsorption direction is shown as downward).

To investigate the adsorption of the H_2O molecules on the surfaces of the defective and the perfect coal molecules, density functional calculations were performed for the 32 adsorption configurations of the H_2O molecules on the surfaces of the three coal molecules. The adsorption energies of the optimized H_2O molecules on the surfaces of the single-vacancy-defective, double-vacancy-defective, and perfect coal molecular models are presented in Tables 2 to 4, respectively. As shown in the tables, the adsorption energies of all the 32 adsorption conformations are negative, indicating that the H_2O molecules have adsorption behavior with each conformation. The adsorption energy of the H_2O molecules in the different conformations by downward adsorption is smaller than that which takes place by upward adsorption. The downward conformation has obvious advantages and is more stable in structure as discussed below. The adsorption energy of H_2O molecules at the adsorption sites **a**, **b**, **c**, and **d** on the surfaces of the single-vacancy-defective coal molecules is less than that of **e**, indicating that wettability at the sites of the defects is stronger. Although the H_2O molecule of configuration **a** is located at the defect, the adsorption of the H_2O molecule at the surface site **a** of the coal molecule is weaker than that of **b**, **c**, and **d** because of the large π system on the surface of the coal molecule. Here, the electron density on the surface is higher than that on the C atom. After the H_2O molecules adsorbed with the surfaces of the single-vacancy-defective coal molecules, the position of the H_2O molecules changed significantly, and the coal molecules all suffered different degrees of deformation, as shown in Figure 7(a−e), corresponding to Figure 6(a−e), respectively. As can be seen, the adsorption stability of H_2O molecules on the single-vacancy-defective coal molecules was much greater than that on the surfaces of the double-vacancy-defective coal molecules and the perfect coal molecules.

The best adsorption sites for the H_2O molecules on the surfaces of the single-vacancy-defective coal molecule, the double-vacancy-defective coal molecule, and the perfect coal

https://doi.org/10.1021/acsomega.2c06146
ACS Omega 2022, 7, 47031−47039

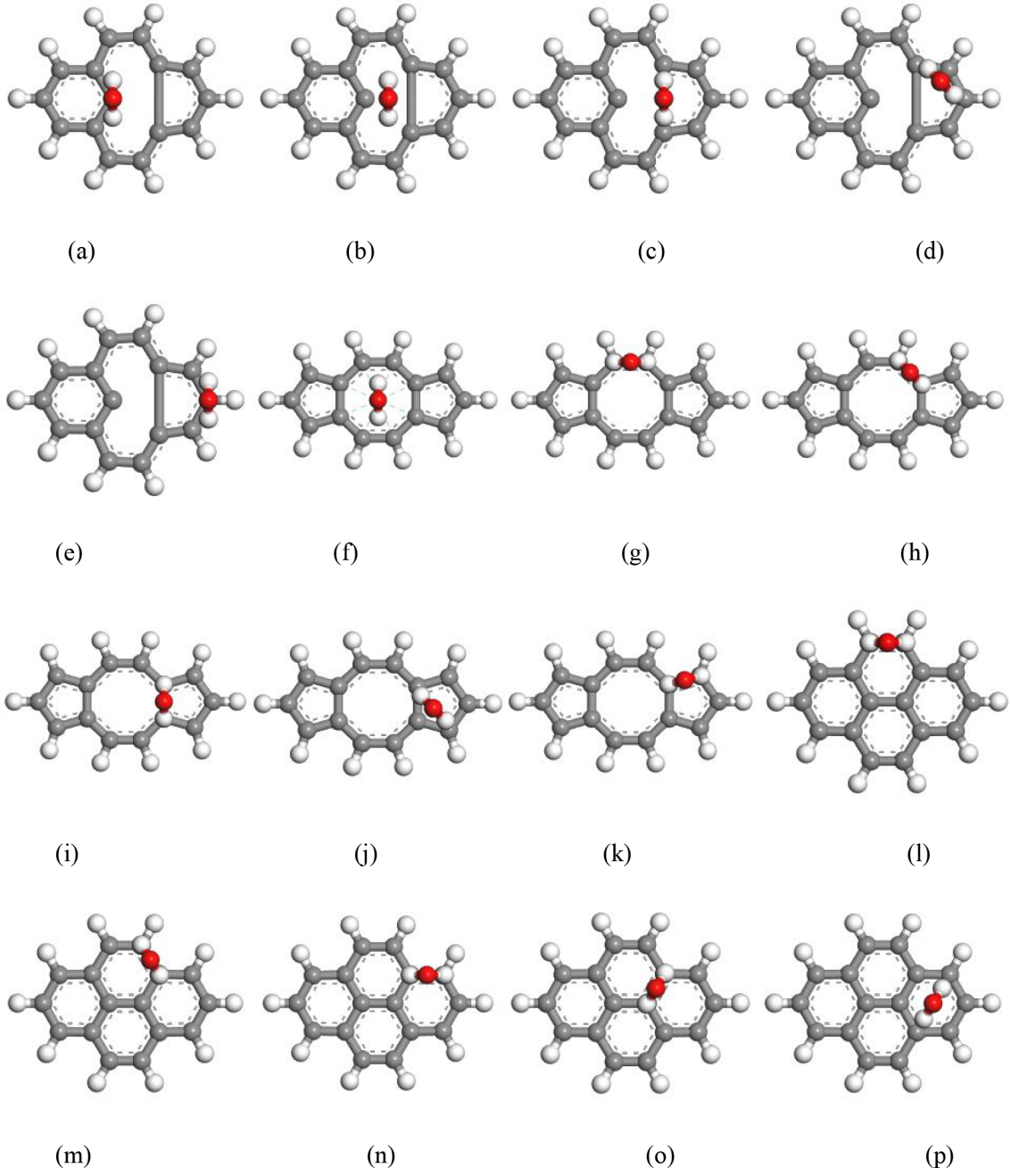

Figure 6. Initial adsorption configurations of the H_2O molecules on the surfaces of the different coal molecular models (downward). (a) H_2O/single-vacancy defect a, (b) H_2O/single-vacancy defect b, (c) H_2O/single-vacancy defect c, (d) H_2O/single-vacancy defect d, (e) H_2O/single-vacancy defect e, (f) H_2O/double-vacancy defect f, (g) H_2O/double-vacancy defect g, (h) H_2O/double-vacancy defect h, (i) H_2O/double-vacancy defect i, (j) H_2O/double-vacancy defect j, (k) H_2O/double-vacancy defect k, (l) H_2O/no-defect l, (m) H_2O/no-defect m, (n) H_2O/no-defect n; (o) H_2O/no-defect o, (p) H_2O/no-defect p.

Table 2. Adsorption Energy of H_2O Molecules on the Surface of the Single-Vacancy-Defective Coal Molecular Model

	Adsorption energy/E_{ads}(kJ·mol^{-1})				
Adsorption mode	Single-vacancy defect a	Single-vacancy defect b	Single-vacancy defect c	Single-vacancy defect d	Single-vacancy defect e
Upward	−31.645	−37.340	−37.209	−36.728	−26.491
Downward	−38.766	−39.319	−39.401	−39.225	−38.603

molecules are **c**, **j**, and **l** sites, corresponding to adsorption energy values of −39.401, −30.002, and −29.844 kJ/mol, respectively. This indicates that the adsorption stability of H_2O molecules on the surfaces of the three coal molecules is greatest in the single-vacancy-defective coal molecule, followed by that of the double-vacancy-defective coal molecule, and then least in the one with no defect. This result is consistent with those obtained from comparing the electronically active degrees in the energy band analysis. Figure 8 illustrates the DOS diagrams of the surfaces of different coal molecules after adsorption of H_2O molecules. In the range of 0−3 eV in the conduction band, the peak surface density of states of single-

https://doi.org/10.1021/acsomega.2c06146
ACS Omega 2022, 7, 47031−47039

Table 3. Adsorption Energy of H_2O Molecules on the Surface of the Double-Vacancy-Defective Coal Molecular Model

	Adsorption energy/E_{ads}(kJ·mol^{-1})					
Adsorption mode	Double-vacancy defect f	Double-vacancy defect g	Double-vacancy defect h	Double-vacancy defect i	Double-vacancy defect j	Double-vacancy defect k
Upward	−8.717	−26.851	−28.516	−6.740	−29.870	−28.975
Downward	−28.463	−27.308	−28.831	−28.749	−30.002	−28.999

Table 4. Adsorption energy of H_2O molecules on the surface of the perfect coal molecular model

	Adsorption energy/E_{ads}(kJ·mol^{-1})				
Adsorption mode	No-defect l	No-defect m	No-defect n	No-defect o	No-defect p
Upward	−26.943	−29.193	−28.878	−27.591	−29.353
Downward	−29.844	−29.364	−28.999	−27.825	−29.605

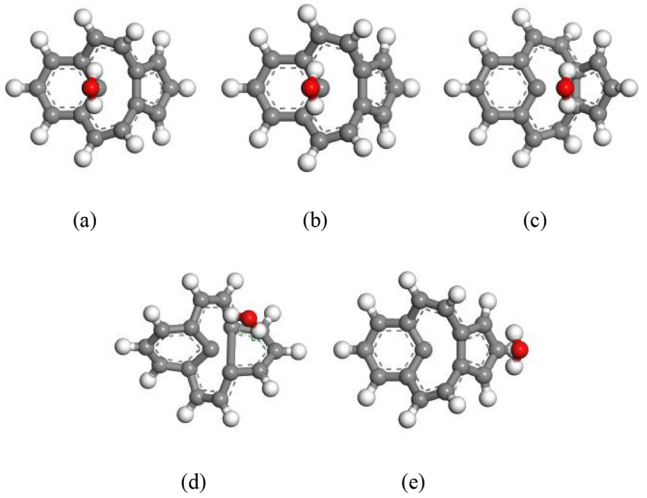

Figure 7. Conformation of H_2O molecule after adsorption on the surface of a single-vacancy-defective coal molecule model (top view). (a) H_2O/single-vacancy defect a, (b) H_2O/single-vacancy defect b, (c) H_2O/single-vacancy defect c, (d) H_2O/single-vacancy defect d, (e) H_2O/single-vacancy defect e.

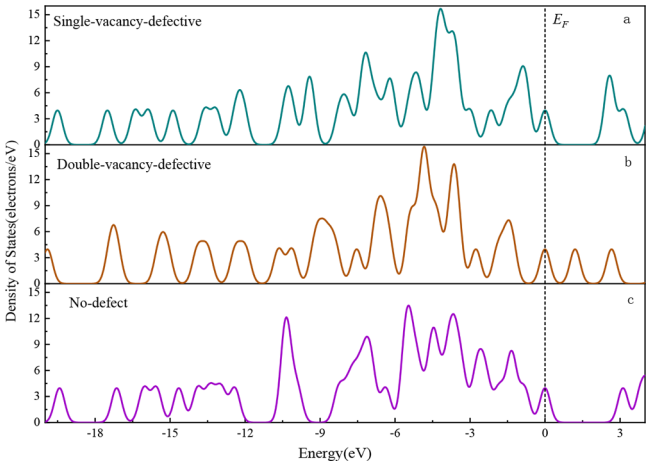

Figure 8. DOS diagrams of the surfaces of different coal molecules after adsorption of H_2O molecules. (a) Single-vacancy-defective coal molecules, (b) double-vacancy-defective coal molecules, (c) no-defect coal molecules.

vacancy-defective coal molecules, double-vacancy-defective coal molecules, and perfect coal molecules are 7.96, 3.95, and 3.91 electrons/eV. The density of states near the Fermi energy level of defective coal molecules is larger, which is consistent with the predicted results.

Figure 9 illustrates the electrostatic potential projection of H_2O molecules in the most stable adsorption conformation of

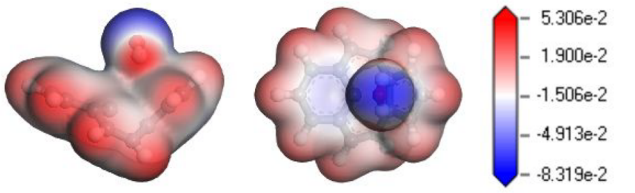

(a) single-vacancy-defective coal molecules (left: side view, right: top view)

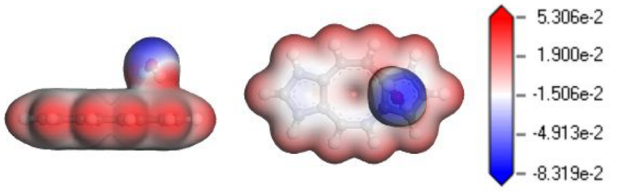

(b) double-vacancy- defective coal molecules (left: side view, right: top view)

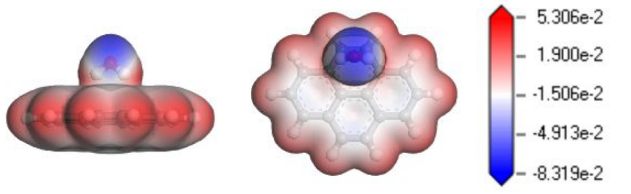

(c) no-defect coal molecules (left: side view, right: top view)

Figure 9. Electrostatic potential projection of H_2O molecules in the most stable conformation of the different coal molecules.

the three coal molecules. The red area represents the positive nature of the charge; the redder the color, the more positive the charge. The blue area represents the negative nature of the charge; the bluer the color, the more negative the charge, and the more electrons that are obtained. As Figure 8 shows, the O atom in the H_2O molecule in the defective coal molecule with single-vacancy defect has less electrostatic potential than that of the perfect coal molecule, with an electrostatic potential value of −0.083 au. The electrostatic potential penetration distance of the H_2O molecule in the defective coal molecule is greater than that of the perfect coal molecule, which indicates

https://doi.org/10.1021/acsomega.2c06146
ACS Omega 2022, 7, 47031−47039

that the H_2O molecule gains more electrons on the surface of the defective coal molecule, and the electrostatic interaction between the two molecules is stronger.

In order to illustrate the adsorption behavior of the two molecules, the Mulliken atomic charges of H_2O molecules on the surfaces of different defective coal models were calculated. Figure 10 illustrates the Mulliken atomic charge transfer

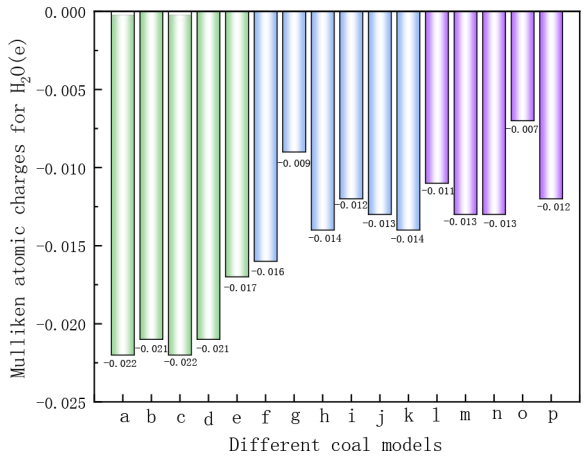

Figure 10. Mulliken charge layout of H_2O molecules adsorbed on the different coal molecular configurations.

between the H_2O molecule and each of the single-vacancy-defective coal molecule, the double-vacancy-defective coal molecule, and the perfect coal molecule model, with positive values indicating loss of electrons and negative values indicating gain of electrons. Since the charge of a single H_2O molecule without interaction is 0 e, the charge of the H_2O molecule adsorbed on the surface of the defective coal model is the charge transferred during the interaction. The more charges transferred, the stronger the adsorption interaction between the two molecules and the more stable the adsorption conformation. The most stable adsorption configurations are those with the lowest adsorption energy. The charges of H_2O molecules in the most stable adsorption configurations of the three coal molecules are −0.022, −0.013, and −0.011 e, respectively, indicating that the H_2O molecules adsorbed more strongly on the surface of the defective coal molecules. These results are consistent with the electrostatic potential projection results. Combined with the adsorption energy calculation results, it can be inferred that the more the charge transferred from the surfaces of coal molecules to H_2O molecules, the smaller the adsorption energy, the more stable the adsorption conformation, and the stronger the wettability.

4. CONCLUSIONS

(1) The results of the energy band structure, TDOS, and electrostatic potential analysis on the surfaces of the different coal molecules show that the surfaces of the defective coal molecules have forbidden bands with narrower widths, smaller electrostatic potential value, and a larger electronic density of states near the Fermi energy level. This means that the surfaces of the defective coal molecules are more electronically active and electron-accumulating than the surfaces of the perfect coal molecules.

(2) The results of frontline orbital analyses of the different coal molecular surface models and H_2O molecules show that the HOMOs of H_2O molecules interact readily with the LUMOs of the different coal molecular models, and the H_2O molecules are more likely to adsorb on the surfaces of the defective coal molecular models.

(3) The results of adsorption energy and charge analysis of H_2O molecules on the surfaces of the different coal molecule models show that the wettability of the H_2O molecules on the surfaces of the three coal molecules is single-vacancy-defective coal molecules > double-vacancy-defective coal molecules > no-defect coal molecules. It is therefore concluded that defects improve the wettability of coal molecule surfaces.

AUTHOR INFORMATION

Corresponding Author

Shuai Wang − *College of Safety Science and Engineering, Liaoning Technical University, Fuxin 123000, China*; Email: zzbganbuke@126.com

Authors

Liyong Tian − *College of Mechanical Engineering, Liaoning Technical University, Fuxin 123000, China*; orcid.org/0000-0001-9532-4179

Xiuyu Yang − *College of Mechanical Engineering, Liaoning Technical University, Fuxin 123000, China*

Ning Yu − *College of Mechanical Engineering, Liaoning Technical University, Fuxin 123000, China*

Complete contact information is available at: https://pubs.acs.org/10.1021/acsomega.2c06146

Notes

The authors declare no competing financial interest.

ACKNOWLEDGMENTS

This work was supported by the National Natural Science Foundation of China(52174143). The authors would like to thank all the reviewers who participated in the review, as well as MJEditor (www.mjeditor.com) for providing English editing services during the preparation of this manuscript.

REFERENCES

(1) Gui, X.; Xing, Y.; Rong, G.; Cao, Y.; Liu, J. Interaction forces between coal and kaolinite particles measured by atomic force microscopy. *Powder Technol.* **2016**, *301*, 349−355.

(2) Liang, L.; Li, Z.; Peng, Y.; Tan, J.; Xie, G. Influence of coal particles on froth stability and flotation performance. *Miner. Eng.* **2015**, *81*, 96−102.

(3) Xia, Y.; Wang, L.; Zhang, R.; Yang, Z.; Xing, Y.; Gui, X.; Cao, Y.; Sun, W. Enhancement of flotation response of fine low-rank coal using positively charged microbubbles. *Fuel* **2019**, *245*, 505−513.

(4) Zhu, G.; Zhang, B.; Zhao, P.; Duan, C.; Zhao, Y.; Zhang, Z.; Yan, G.; Zhu, X.; Ding, W.; Rao, Z. Upgrading low-quality oil shale using high-density gas-solid fluidized bed. *Fuel* **2019**, *252*, 666−674.

(5) Sivrikaya, O. Cleaning study of a low-rank lignite with DMS, Reichert spiral and flotation. *Fuel* **2014**, *119*, 252−258.

(6) Sakaguchi, M.; Laursen, K.; Nakagawa, H.; Miura, K. Hydrothermal upgrading of Loy Yang Brown coal-Effect of upgrading conditions on the characteristics of the products. *Fuel Process. Technol.* **2008**, *89*, 391−396.

(7) Gui, X.; Xing, Y.; Rong, G.; Cao, Y.; Liu, J. Interaction forces between coal and kaolinite particles measured by atomic force microscopy. *Powder Technol.* **2016**, *301*, 349−355.

https://doi.org/10.1021/acsomega.2c06146
ACS Omega 2022, 7, 47031−47039

(8) Verrelli, D.; Koh, P.; Nguyen, A. Particle-bubble interaction and attachment in flotation. *Chem. Eng. Sci.* **2011**, *66*, 5910−5921.
(9) Crawford, R.; Guy, D.; Mainwaring, D. The influence of coal rank and mineral matter content on contact angle hysteresis. *Fuel* **1994**, *73*, 742−746.
(10) Huo, Y.; Zhu, H.; He, X.; Fang, S.; Wang, W. Quantum Chemical Calculation of the Effects of H_2O on Oxygen Functional Groups during Coal Spontaneous Combustion. *ACS Omega* **2021**, *6*, 25594−25607.
(11) Zhou, G.; Xu, C.; Cheng, W.; Zhang, Q.; Nie, W. Effects of Oxygen Element and Oxygen-Containing Functional Groups on Surface Wettability of Coal Dust with Various Metamorphic Degrees Based on XPS Experiment. *J. Anal. Methods Chem.* **2015**, *2015*, 1−8.
(12) Zhang, R.; Xia, Y.; Guo, F.; Sun, W.; Cheng, H.; Xing, Y.; Gui, X. Effect of microemulsion on low-rank coal flotation by mixing DTAB and diesel oil. *Fuel* **2020**, *260*, 116321.
(13) Zhang, J.; Liu, K.; Clennell, M.; Dewhurst, D.; Pervukhina, M. Molecular simulation of CO_2/CH_4 competitive adsorption and induced coal swelling. *Fuel* **2015**, *160*, 309−317.
(14) Zhao, Y.; Feng, Y.; Zhang, X. Molecular simulation of CO_2/CH_4 self and transport diffusion coefficients in coal. *Fuel* **2016**, *165*, 19−27.
(15) Hu, H.; Li, X.; Fang, Z.; Wei, N.; Li, Q. Small-molecule gas sorption and diffusion in coal: Molecular simulation. *Energy* **2010**, *35*, 2939−2944.
(16) Van Niekerk, D.; Mathews, J. Molecular dynamic simulation of coal-solvent interactions in Permian-aged South African coals. *Fuel Process. Technol.* **2011**, *92*, 729−734.
(17) Xia, Y.; Zhang, R.; Cao, Y.; Xing, Y.; Gui, X. Role of molecular simulation in understanding the mechanism of low-rank coal flotation: A review. *Fuel* **2020**, *262*, 116535.
(18) Zhang, R.; Xing, Y.; Xia, Y.; Luo, J.; Tan, J.; Rong, G.; Gui, X. New insight into surface wetting of coal with varying coalification degree: An eperimental and molecular dynamics simulation study. *Appl. Surf. Sci.* **2020**, *511*, 145610.
(19) Xia, Y.; Yang, Z.; Zhang, R.; Xing, Y.; Gui, X. Enhancement of the surface hydrophobicity of low-rank coal by adsorbing DTAB: An experimental and molecular dynamics simulation study. *Fuel* **2019**, *239*, 145−152.
(20) Wang, C.; Xing, Y.; Xia, Y.; Zhang, R.; Wang, S.; Shi, K.; Tan, J.; Gui, X. Investigation of interactions between oxygen-containing groups and water molecules on coal surfaces using density functional theory. *Fuel* **2021**, *287*, 119556.
(21) Pinheiro, M.; Cardoso, D. V. V.; Aquino, A. J. A.; Machado, F. B. C.; Lischka, H. The characterization of electronic defect states of single and double carbon vacancies in graphene sheets using molecular density functional theory. *Mol. Phys.* **2019**, *117*, 1519−1531.
(22) Zhuang, H.; Johannes, M.; Blonsky, M.; Hennig, R. Computational prediction and characterization of single-layer CrS2. *Appl. Phys. Lett.* **2014**, *104*, 022116.
(23) Shakeri, M. Effect of randomly distributed asymmetric stone-wales defect on electronic and transport properties of armchair graphene nanoribbon. *Superlattice. Microst.* **2019**, *128*, 116−126.
(24) Guo, D.; Guo, X.; Chen, P.; Liu, Q. Influence of dynamic damage of deformed coal molecular structure on methane adsorption. *J. China Coal Soc.* **2020**, *45*, 2610−2618.
(25) del Castillo, R. M.; Calles, A. G.; Espejel-Morales, R.; Hernandez-Coronado, H. Adsorption of CO_2 on graphene surface modified with defects. *Comput. Condens. Matte.* **2018**, *16*, e00315.
(26) Gensterblum, Y.; Busch, A.; Krooss, B. Molecular concept and experimental evidence of competitive adsorption of H_2O, CO_2 and CH_4 on organic material. *Fuel* **2014**, *115*, 581−588.
(27) Mosher, K.; He, J.; Liu, Y.; Rupp, E.; Wilcox, J. Molecular simulation of methane adsorption in micro- and mesoporous carbons with applications to coal and gas shale systems. *Int. J. Coal Geol.* **2013**, *109−110*, 36−44.
(28) Hao, S.; Wen, J.; Yu, X.; Chu, W. Effect of the surface oxygen groups on methane adsorption on coals. *Appl. Surf. Sci.* **2013**, *264*, 433−442.
(29) Qiu, N.; Xue, Y.; Guo, Y.; Sun, W.; Chu, W. Adsorption of methane on carbon models of coal surface studied by the density functional theory including dispersion correction (DFT-D3). *Comput. Theor. Chem.* **2012**, *992*, 37−47.
(30) Cheng, G.; Li, Y.; Zhang, M.; Cao, Y. Simulation of the adsorption behavior of $CO_2/N_2/O_2$ and H_2O molecules in lignite. *J. China Coal Soc.* **2021**, *46*, 960−969.
(31) Zhou, Y.; Sun, W.; Chu, W.; Liu, X.; Jing, F.; Xue, Y. Theoretical insight into the enhanced CH_4 desorption via H_2O adsorption on different rank coal surfaces. *J. Energy Chem.* **2016**, *25*, 677−682.
(32) Perdew, J.; Burke, K.; Ernzerhof, M. Generalized gradient approximation made simple. *Phys. Rev. Lett.* **1996**, *77*, 3865−3868.
(33) Chen, J.; Min, F.; Liu, L.; Peng, C. DFT calculations of different amine /ammonium cations adsorption on kaolinite (001) surface. *J. China Coal Soc.* **2016**, *41*, 3115−3121.
(34) Han, Y.; Liu, W.; Chen, J.; Han, Y. Adsorption mechanism of hydroxyl calcium on two kaolinite (001) surface. *J. China Coal Soc.* **2016**, *41*, 743−750.
(35) Clark, S.; Segall, M.; Pickard, C.; Hasnip, P.; Probert, M.; Refson, K.; Payne, M. First principles methods using CASTEP. *Z. Kristallogr.* **2005**, *220*, 567−570.
(36) Vanderbilt, D. Soft self-consistent pseudopotentials in a generalized eigenvalue formalism. *Phys. Rev. B* **1990**, *41*, 7892−7895.
(37) Talla, J. Band gap tuning of defective silicon carbide nanotubes under external electric field: density functional theory. *Phys. Lett. A* **2019**, *383*, 2076−2081.
(38) Zribi, B.; Haghiri-Gosnet, A.; Bendounan, A.; Ouerghi, A.; Korri-Youssoufi, H. Charge transfer and band gap opening of a ferrocene/graphene heterostructure. *Carbon* **2019**, *153*, 557−564.
(39) Qi, X.; Zhang, H.; Li, Y.; Chen, J. Density functional theory study of the structure and properties of C-doped pyrite. *Physica B* **2019**, *572*, 168−174.
(40) Wang, C.; Xing, Y.; Xia, Y.; Chen, P.; Chen, W.; Tan, J.; Zhang, C.; Gui, X. Effect of vacancy defects on electronic properties and wettability of coal surface. *Appl. Surf. Sci.* **2020**, *511*, 145546.
(41) Zhang, Y.; An, L.; Fan, Q.; Chen, T. First principles study on adsorption of Co^2+ on vacancy-defected and boron-doped graphene. *Chin. J. Nonferr. Metal.* **2022**, *32*, 139−147.
(42) Zhao, D.; Liu, X. Density functional calculation of $H_2O/CO_2/CH_4$ for oxygen-containing functional groups in coal molecules. *ACS Omega* **2022**, *7*, 17330−17338.
(43) Zhao, Z.; Wang, G.; Zhai, P.; Qi, C.; Chen, X. Study on Adsorption Behavior of N_2 and O_2 on δ-Pu (100) Surface Based on Density Functional Theory. *J. S. China Norm. Univ.* **2022**, *54*, 1−8.
(44) Chen, J.; Min, F.; Liu, L. Density Function Study on Microscopic Interactions Between Fine Particles of Coal and Kaolinite in Coal Slurry Water. *Mater. Rep.* **2019**, *33*, 2677−2683.
(45) Chen, J.; Min, F.; Liu, L.; Cai, C. Systematic exploration of the interactions between Fe-doped kaolinite and coal based on DFT calculations. *Fuel.* **2020**, *266*, 117082.
(46) Lin, B.; Li, Y.; Yang, K.; Kong, J.; Zhang, X. Competitive adsorption mechanism of H_2O and CH_4 on coal surface. *J. Xi'An Univ. Sci. Technol.* **2018**, *38* (6), 878−885.

https://doi.org/10.1021/acsomega.2c06146
ACS Omega 2022, 7, 47031−47039